Force acting on the Vertical Structure during Overflow

CIVIL & ENVIRONMENTAL ENGINEERING UNIVERSITY OF MICHIGAN

Session P25

Taeksang Kim[1], Julien Malherbe[1], Sirawit Shimpalee[2], Stefan Felder[3] and Jeremy Bricker[1,4]

[1] Civil and Environmental Engineering, University of Michigan, 2350 Hayward St, Ann Arbor, MI, 48109, USA, [2] Naval Architecture and Marine Engineering, University of Michigan, 2600 Draper Drive, Ann Arbor, MI, 48109, USA,
[3] School of Civil and Environmental Engineering, UNSW Sydney, 110 King St, Manly Vale, NSW, 2093, Australia, [4] Hydraulic Engineering, Delft University of Technology, 2628 CN, Delft, the Netherlands

1. Introduction

▶ Research necessity

- Overflow scenarios introduce complex challenges related to jet trajectories and air entrainment, demanding meticulous study.
- Existing analyses frequently overlook essential factors, especially sub-atmospheric pressure in the cavity, which can jeopardize structural stability.
- Moreover, current research reveals inaccuracies in calculating downstream water forces due to assumption of hydrostatic pressure, neglecting the influence of significant air bubble movement in air-water flows

▶ Research objectives

- Investigate the intricate fluid dynamics of air-water flow and cavity pressure properties during vertical structure overflow.
- Utilize experiments to quantify the force acting on the model vertical structure, using different water pressure profiles: 1) Hydrostatic, 2) Bernoulli, 3) Discretized Navier-Stokes.
- Utilize the Buckingham Pi theorem to establish non-dimensional relationships among variables for convenient application of the research findings.

2. Key Concepts

▶ Background review: air entrainment mechanism (with Aerated and Non-aerated cases)

- As shown in Figure 1, according to Chanson (1996), air bubble entrainment occurs along the cavity interface and at the end of the cavity through a re-entrant jet mechanism, leading to negative pressure in the air cavity.

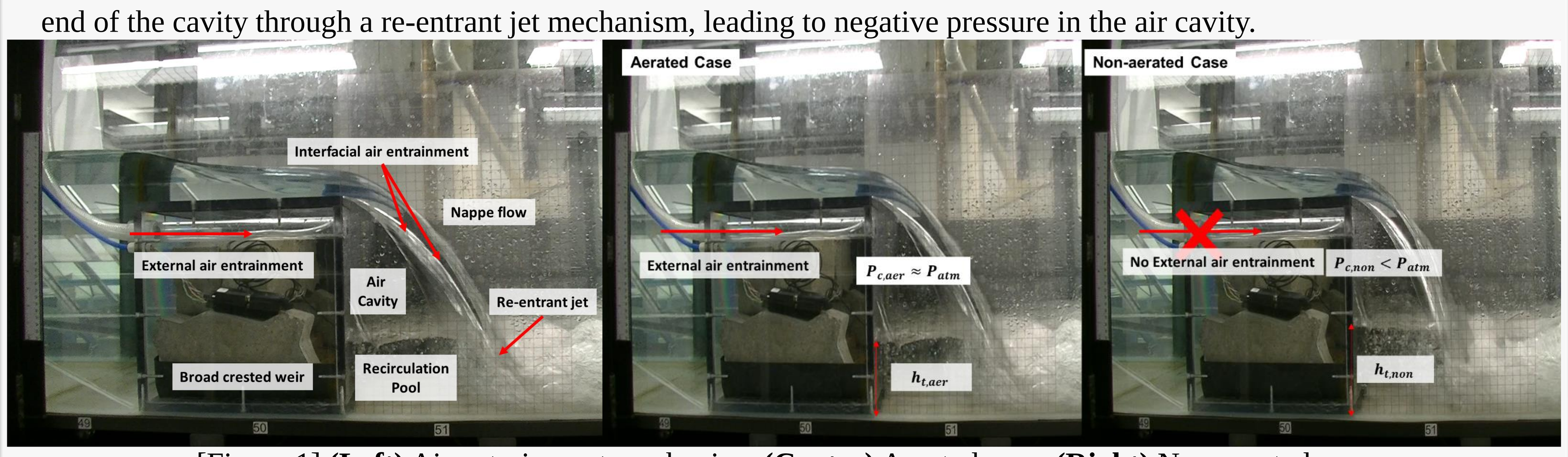

[Figure 1] **(Left)** Air entrainment mechanism **(Center)** Aerated case, **(Right)** Non-aerated case
Reference: Chanson, H. (1996). *Air bubble entrainment in free-surface turbulent shear flows*. Elsevier.

▶ Pressure acting on the structure

- Upstream: Hydrostatic Pressure
- Downstream: Cavity pressure + Navier Stokes

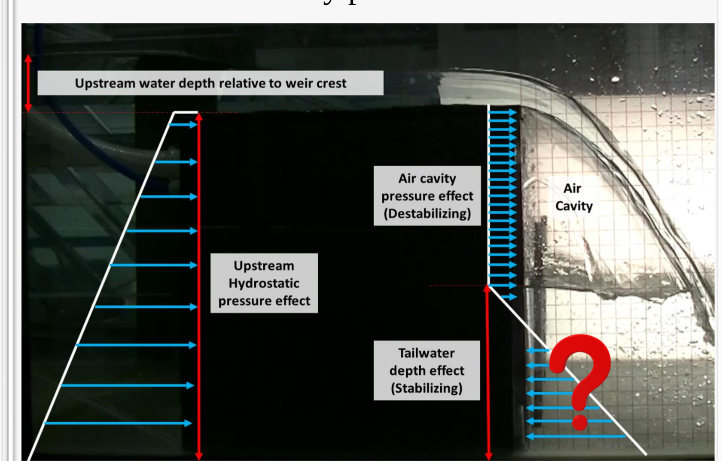

[Figure 2] Pressure Profile distribution

▶ Downstream flow regime

- The pattern of air cavity pressure and air-water pressure may differ with changes in the downstream flow regime conditions.

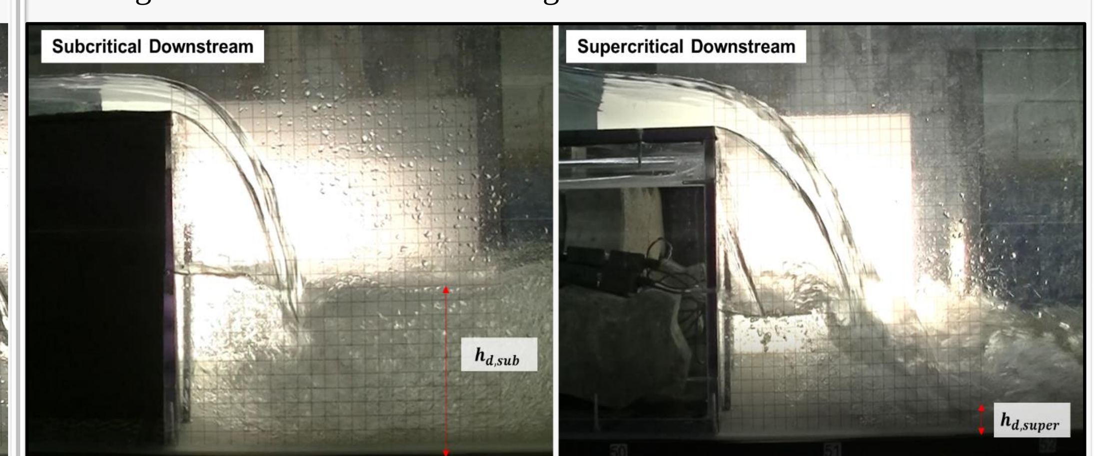

[Figure 3] Downstream flow regime (**Left**: Subcritical, **Right**: Supercritical)

3. Research Methodology

▶ Experimental setup: Flume and model weir

- As shown in Figure 1, air bubble entrainment occurs along the cavity interface and at the end of the cavity through a re-entrant jet mechanism, leading to negative pressure in the air cavity.

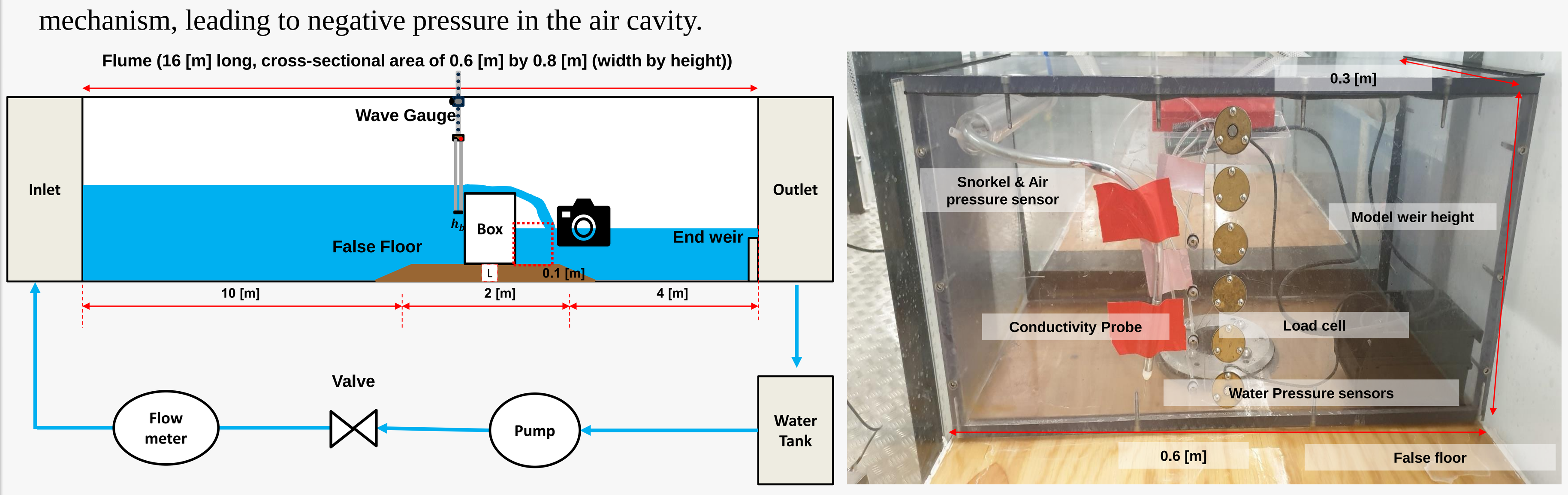

[Figure 4] **(Left)** Side view of the flume that used in the experiment, **(Right)** Downstream face of the model weir

▶ Experimental variables

- The number of total experimental cases: 192 cases with different independent variables.
- Independent variables and dependent variables are detailed in Table 1.

Variables	Values	Unit	How to measure?
Flow discharge	8 different cases	$[lpm]$	Flowmeter
Model weir height	(0.3, 0.35, 0.4)	$[m]$	Constants
End weir height	(0, 0.05, 0.10, 0.15)	$[m]$	Constants
Cavity aeration	Aerated or Non-aerated	–	–
Upstream water depth relative to weir crest	Dependent	$[m]$	Gauge Sensor
Air-water density	Dependent	$[kg/m^3]$	Conductivity Probe
Air cavity pressure and air-water pressure	Dependent	$[Pa]$	Pressure sensor
Tailwater depth	Dependent	$[m]$	Image processing method
Velocity close to the wall	Dependent	$[m/s]$	BIV method
Force acting on the box	Dependent	$[N]$	Load Cell

[Table 1] Independent variables (in black) and dependent variables (in blue)

▶ Mathematical expression for different pressure profiles

- Applying hydrostatic conditions is incorrect due to air bubble movement.
- In this study, we calculate and integrate 1) Hydrostatic, 2) Bernoulli, and 3) Navier-stokes pressure, respectively, to determine the forces acting on the model
- Find the pressure profile that best matches the measured force.
- For Hydrostatic condition: Assuming steady, uniform, and inviscid conditions

$$\left(\frac{\partial v}{\partial t} + u\frac{\partial v}{\partial x} + v\frac{\partial v}{\partial y}\right) = -\frac{1}{\rho_m}\frac{\partial p}{\partial y} + v_t\left(\frac{\partial^2 v}{\partial x^2} + \frac{\partial^2 v}{\partial y^2}\right) - g \quad \rightarrow \quad p_h = -\rho_m g y$$

- For Bernoulli equation: Assuming steady and inviscid conditions

$$\left(\frac{\partial v}{\partial t} + u\frac{\partial v}{\partial x} + v\frac{\partial v}{\partial y}\right) = -\frac{1}{\rho_m}\frac{\partial p}{\partial y} + v_t\left(\frac{\partial^2 v}{\partial x^2} + \frac{\partial^2 v}{\partial y^2}\right) - g \quad \rightarrow \quad \frac{p_b}{\rho_m g} + \frac{V^2}{2g} + y = C$$

- For Navier-Stokes equation:

$$\left(\frac{\partial v}{\partial t} + u\frac{\partial v}{\partial x} + v\frac{\partial v}{\partial y}\right) = -\frac{1}{\rho_m}\frac{\partial p_n}{\partial y} + v_t\left(\frac{\partial^2 v}{\partial x^2} + \frac{\partial^2 v}{\partial y^2}\right) - g$$

(FDM with Forward-time and Forward or Backward space scheme is used)

▶ Velocity calculation

- Velocity calculations employed the Bubble Image Velocimetry (BIV) method from the PIVlab MATLAB toolbox.
- High-speed videos (120 fps) were used to capture bubble motion.
- A QR code provides access to a video demonstration. (Top: Aerated, Bottom: Non-aerated)

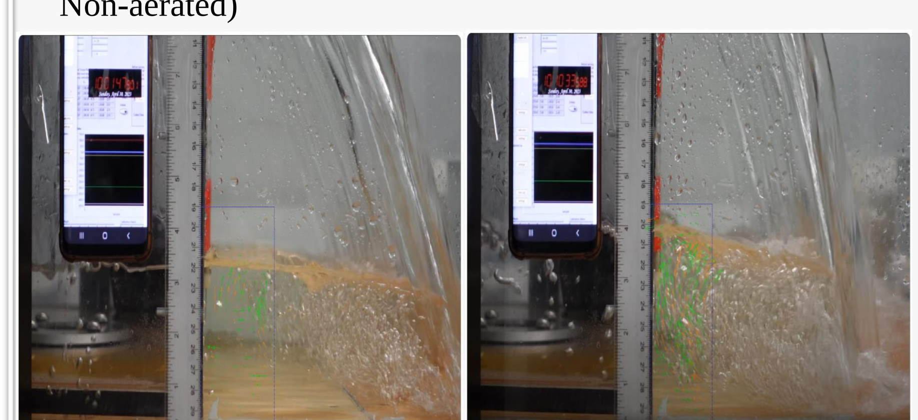

[Figure 5] Snapshot of velocity vectors (**Left**: Aerated, **Right**: Non-aerated)

▶ Tailwater depth calculation

- Object Tracking was utilized for fluctuating tailwater depth calculations, combining color threshold, edge detection, and the mean-shift tracking algorithm.
- A QR code provides access to a video demonstration. (Top: Aerated, Bottom: Non-aerated)

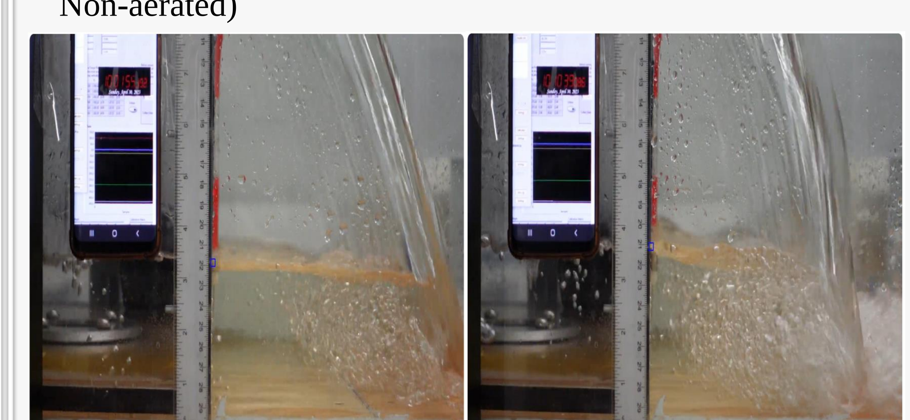

[Figure 6] Snapshot of Tailwater depth (**Left**: Aerated, **Right**: Non-aerated)

4. Research Results

▶ Data acquisition results

- All data, including cavity pressure, air-water pressure, discharge, water depth, velocity, and more, were collected over a 30-second duration. To facilitate visualization, the sampling rate was standardized to 10 Hz.
- There are noticeable differences between an aerated case and a non-aerated case, particularly in terms of cavity pressure.

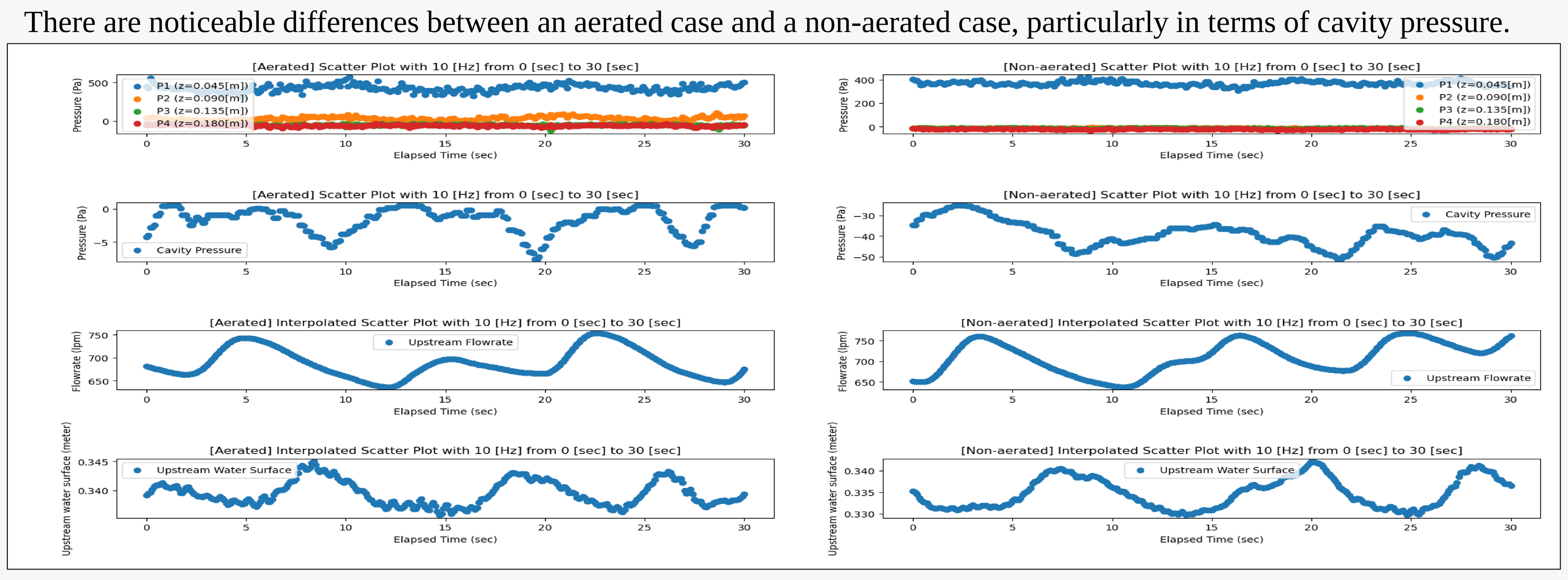

[Figure 7] Air-Water Pressure, Cavity Pressure, Discharge, and Upstream Water Depth (**Left**: Aerated, **Right**: Non-aerated)

▶ Dimensionless equation for air-cavity pressure with different downstream flow regime

- Subcritical downstream flow:

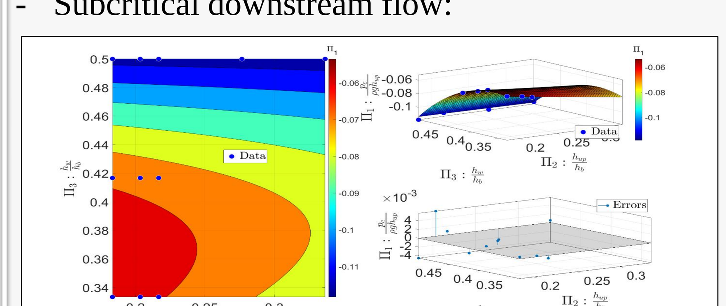

Dimensionless parameters		Dimensionless Equation			
$\Pi_1: \frac{p_c}{\rho g h_{up}}$ $\Pi_2: \frac{h_{up}}{h_b}$ $\Pi_3: \frac{h_w}{h_b}$		$\Pi_1 = C_{00} + C_{10}\Pi_2 + C_{01}\Pi_3 + C_{11}\Pi_2\Pi_3 + C_{02}(\Pi_3)^2$			
Goodness of fit		Coefficients with 95% confidence bounds			
		Coefficients	Avg.	Lower bound	Upper bound
SSE	0.000	C_{00}	-0.37	-0.59	-0.14
R-squared	0.992	C_{10}	-0.44	-1.35	0.48
Adjusted R-squared	0.987	C_{01}	2.05	1.30	2.80
RMSE	0.003	C_{11}	0.85	-1.01	2.71
		C_{02}	-3.08	-3.88	-2.27

- Supercritical downstream flow:

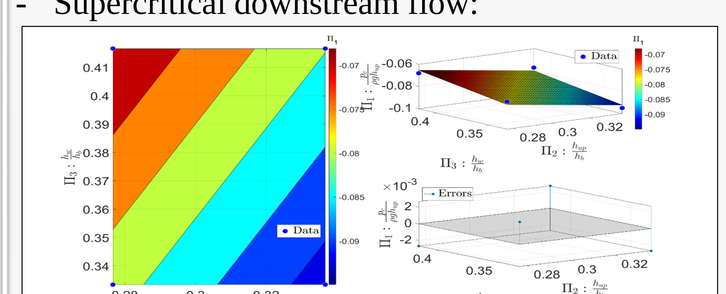

Dimensionless parameters		Dimensionless Equation			
$\Pi_1: \frac{p_c}{\rho g h_{up}}$ $\Pi_2: \frac{h_{up}}{h_b}$ $\Pi_3: \frac{h_w}{h_b}$		$\Pi_1 = C_{00} + C_{10}\Pi_2 + C_{01}\Pi_3$			
Goodness of fit		Coefficients with 95% confidence bounds			
		Coefficients	Average value	Lower bound	Upper bound
SSE	0.000	C_{00}	-0.06	-0.53	0.40
R-squared	0.927	C_{10}	-0.24	-1.37	0.89
Adjusted R-squared	0.781	C_{01}	0.15	-0.66	0.96
RMSE	0.005				

[Figure 8] Dimensionless equations for air cavity pressure (**Top**: Subcritical downstream, **Bottom**: Supercritical downstream)

▶ Pressure profile and tailwater depth at downstream wall of the model weir

- Bernoulli and Navier-Stokes pressures tend to align, but there are differences compared to hydrostatic pressure. This suggests that the velocity term significantly influences pressure in this sheet flow.
- You can access a real-time pressure data video demonstration through a QR code (Top: Aerated, Bottom: Non-aerated).

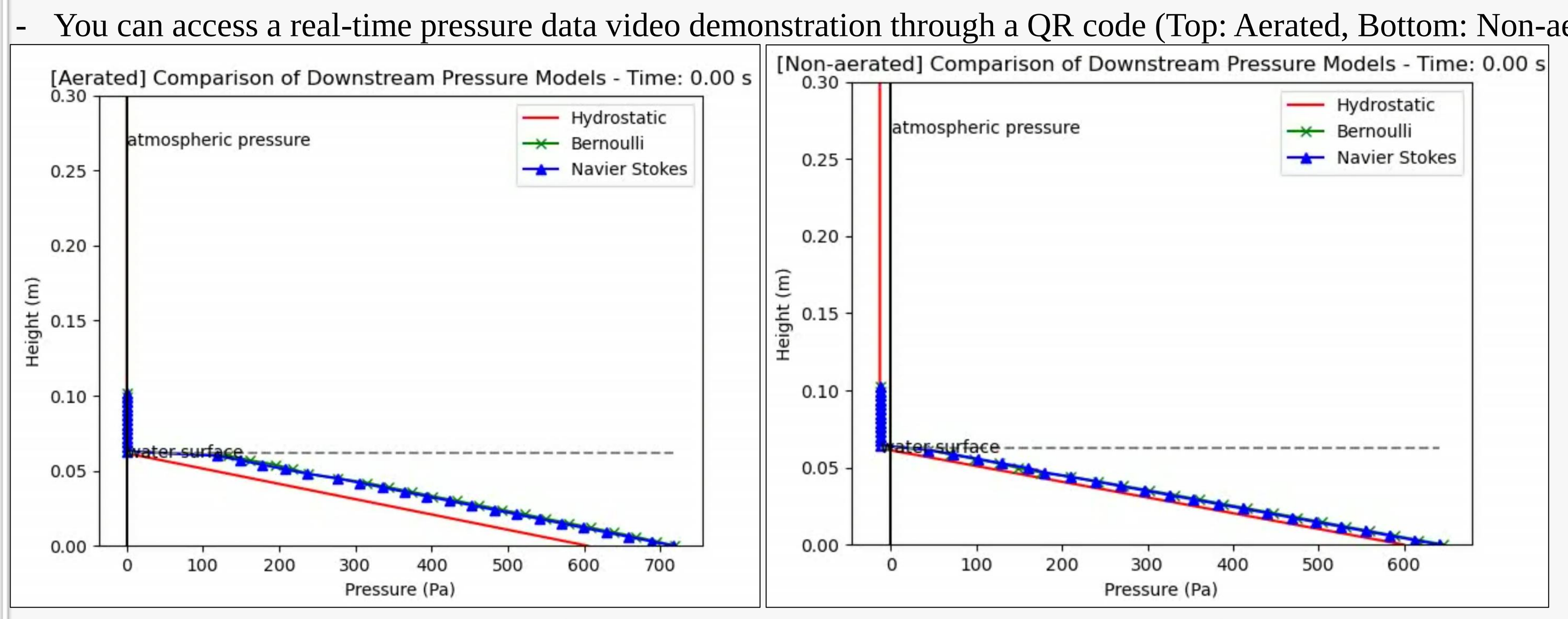

[Figure 9] Contrasting pressure profiles and tailwater depth at downstream wall (**Left**: Aerated, **Right**: Non-aerated)

▶ Force acting on the model weir

- Real-time forces obtained from various pressure profiles (Red: Hydrostatic, Green: Bernoulli, Blue: Navier-Stokes).
- Navier-Stokes forces (Blue line) consistently align with measured values (Black line), regardless of aeration or flow rate.

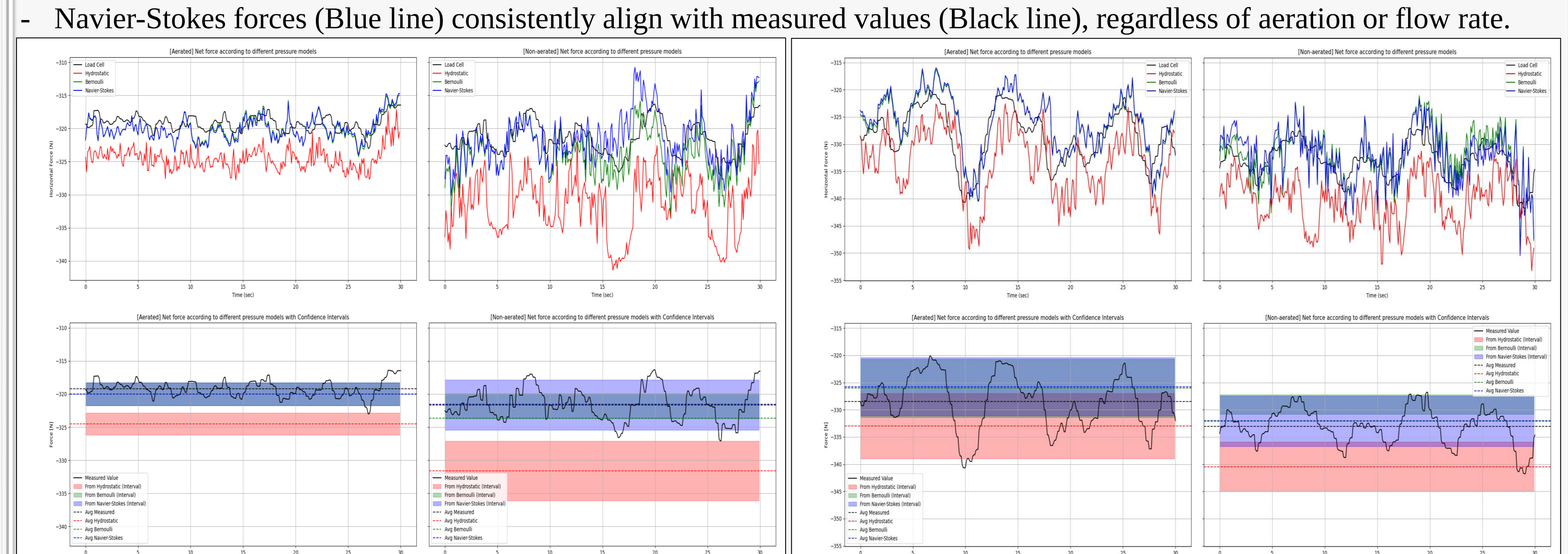

[Figure 10] Net force acting on the model weir (**Left**: low flowrate, **Right**: high flowrate)

5. Conclusions

1. There are significant differences between the aerated and non-aerated cases in terms of factors such as air cavity pressure, tailwater depth, and the forces acting on the box.
2. In subcritical and supercritical downstream scenarios, there exist distinct relationships between air cavity pressure and independent variables.
3. In overflow scenarios like this study, it has been verified through comparisons with measured data that to accurately determine the pressure acting on the downstream wall, the Navier-Stokes equation must be utilized.